Decomposition of γ-Cyclotrimethylene Trinitramine (γ-RDX): Relevance for Shock Wave Initiation

ARTICLE *in* THE JOURNAL OF PHYSICAL CHEMISTRY A · AUGUST 2012

Impact Factor: 2.69 · DOI: 10.1021/jp306589h · Source: PubMed

2 AUTHORS, INCLUDING:

Zbigniew Dreger
Washington State University
124 PUBLICATIONS **1,127** CITATIONS

SEE PROFILE

THE JOURNAL OF PHYSICAL CHEMISTRY A

Article

pubs.acs.org/JPCA

Decomposition of γ-Cyclotrimethylene Trinitramine (γ-RDX): Relevance for Shock Wave Initiation

Zbigniew A. Dreger* and Yogendra M. Gupta

Institute for Shock Physics and Department of Physics, Washington State University, Pullman, Washington 99164-2816, United States

ABSTRACT: To elucidate the reactive behavior of RDX crystals at pressures and temperatures relevant to shock wave initiation, Raman spectroscopy and optical imaging were used to determine the pressure−temperature ($P-T$) stability and the decomposition of γ-RDX, the high pressure phase of RDX. Experiments were performed on single crystals in a diamond anvil cell at pressures from 6 to 12 GPa and at temperatures up to 600 K. Evidence for the direct decomposition of γ-RDX above 6 GPa, without the involvement of other phases, is provided. The upper limit of the $P-T$ locus for the γ-RDX thermal decomposition was determined. A refined $P-T$ phase diagram of RDX is presented that includes the current findings for γ-RDX. The static compression results are used to gain key insight into the shock initiation of RDX, including a determination of the RDX phase at decomposition and understanding the role of pressure and temperature in accelerating shock induced decomposition. This study has established the important role that γ-RDX plays in decomposition of RDX under static and shock compression conditions; thus theoretical modeling of RDX decomposition at high pressures and temperatures needs to incorporate the γ-phase response.

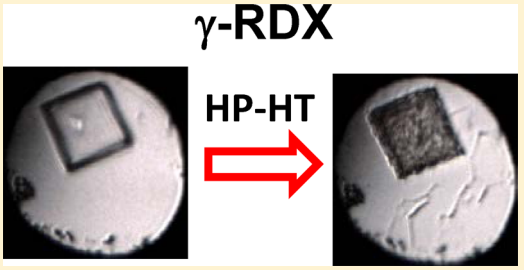

1. INTRODUCTION

RDX ($(CH_2NNO_2)_3$), a cyclic trimer of methylenenitramine, is an important energetic crystal due to its wide use in explosives and monopropellants. Because practical applications of this material often involve shock wave loading, RDX properties and performance at thermo-mechanical conditions relevant to shock wave initiation are of particular interest. Despite the significant differences in loading rates, static high pressure and high temperature (HP-HT) experiments provide key results regarding the reactive behavior of energetic crystals at pressures and temperatures relevant to shock wave initiation. As demonstrated in our previous work on shock compressed RDX crystals, static compression results are needed to gain insight into molecular processes under shock compression. For instance, we established that the same $\alpha-\gamma$ phase transition, which was previously identified under static compression, also takes place under shock compression.[1−3] However, to benefit fully from static compression studies, reliable and more complete data at high pressures and high temperatures, relevant to shock initiation conditions, are needed.

Recently, considerable progress has been made in elucidating the HP-HT behavior of RDX.[4−7] A new phase diagram, to 7 GPa and 550 K, was determined, which defined the boundaries between the α- and γ-RDX, and the phase that is formed exclusively at the HP-HT conditions.[4] The $\alpha-\gamma$ phase transition was confirmed to take place at ∼4 GPa regardless of temperatures from 297 to 466 K. The HP-HT phase was identified as a new phase, ε-RDX,[5,6] in contrast to earlier suggestions that it was β-RDX,[8,9] usually observed at ambient pressure.[7,10,11] It was also established that ε-RDX has limited stability at high pressures and high temperatures and decomposes readily according to an autocatalytic rate law.[4] Importantly, this phase was found to be formed only in a narrow domain of pressures (from 2.8 to 6 GPa) and temperatures (above 466 K).[4]

Despite the advances indicated above, the current understanding of the RDX behavior at static HP-HT is not sufficient, particularly at higher pressures. Our finding[4] that ε-RDX is constrained to pressures below 6 GPa brings into question previous claims that (i) ε-RDX is primarily responsible for RDX decomposition under the HP-HT conditions[8,9] and (ii) γ-RDX only decomposes at high temperatures with prior transformation to ε-RDX.[9] In this work, we address these issues by examining the thermal decomposition of RDX at pressures above 6 GPa. Because shock initiation of RDX takes place at pressures above ∼5−6 GPa,[12] results of the present study are of particular interest for understanding shock-induced decomposition.[12,13]

As in our previous work,[4,5] we use the HP-HT vibrational spectroscopy measurements along with optical imaging to examine the chemical stability and decomposition of RDX single crystals. The specific objectives of this work were: (1) to determine the stability of γ-RDX, (2) to establish the role of γ-RDX in the HP-HT decomposition of RDX, and (3) to relate the static compression results to shock compression data. Our experimental data are expected to be valuable for theoretical/computational modeling of the HP-HT decomposition of RDX.

Received: July 3, 2012
Revised: August 3, 2012
Published: August 9, 2012

   dx.doi.org/10.1021/jp306589h | J. Phys. Chem. A 2012, 116, 8713−8717

The remainder of this paper is organized as follows. Experimental procedures including sample preparation, high-pressure generation, and HP-HT Raman measurements are described briefly in the next section. Section 3 presents experimental data and discussion regarding the three objectives listed above. The main findings of this work are summarized in section 4.

2. EXPERIMENTAL METHODS

Small single crystals of RDX were grown from an acetone solution using RDX polycrystals provided by Dr. D. E. Hooks of Los Alamos National Laboratory. The crystals were carefully selected to ensure similar size and quality. Crystal quality was evaluated using an optical microscope (160X), and only the crystals that were free of observable microscopic defects were used. Typical samples had a square shape and approximate dimensions of $(80 \times 80 \times 30)\ \mu m^3$ to fill only a fraction of the high pressure cell compartment.

High pressures were produced using a modified Merrill-Bassett type diamond-anvil-cell (DAC). A spring-steel gasket, preindented to 0.06−0.08 mm with a 0.125 or 0.200 mm hole drilled in the indentation, was used as a sample compartment. A single crystal of RDX and a ruby chip were loaded into the sample compartment. As in our previous experiments,[4,5] cryogenically loaded argon was used as an inert pressure transmitting medium. The crystal quality was not affected upon cryogenic loading, as was indicated by the same shape of Raman spectra and the same appearance of sample in optical images. The ruby fluorescence method utilizing R-line shifts was used to monitor pressure.[14] The precision of our pressure measurements at room temperature was estimated to be 0.05 GPa.

The temperature of the DAC was varied by using a resistive heater wrapped around the cell. The sample temperature was monitored using iron−constantan thermocouples. Two thermocouples were positioned on the facets of the diamond anvil, close to the diamond culet, and displaced from each other by about 180°. In controlled experiments, these two thermocouples were calibrated with respect to a thermocouple placed into the gasket hole to provide the necessary adjustment for determining the sample temperature. The accuracy of the temperature measurements in our experiments was estimated to be ±2 K and was determined as a standard deviation from several controlling experiments.

A micro-Raman system (T64000, JY-Horiba) equipped with a microscope (Olympus BX-40) was used to provide the spectra and images of γ-RDX at various pressures and temperatures. The 532 nm line from a continuous wave (cw) diode-pumped solid-state (DPSS) laser (Verdi-Coherent) was employed for Raman excitation. To avoid any irreversible effects in the sample, the exposure time and the laser irradiation power were kept at a low level. Specifically, the incident power on the sample did not exceed 50 mW, and the accumulation time of the Raman spectra was usually 2 s. Furthermore, the size of the laser spot was adjusted to acquire signal from most of the sample. Experimental details regarding our micro-Raman and ruby fluorescence measurement techniques can be found elsewhere.[3−5]

Raman experiments were carried out at pressures ranging from 6 to 12 GPa, and at temperatures ranging from ∼295 to 600 K. Measurements were performed at increasing temperatures to determine the pressure and temperature locus for the γ-RDX thermal decomposition. In these experiments, for any given pressure, the RDX crystals were heated from room temperature to 600 K at a constant rate of 1 K/min. The Raman spectra and/or optical images were acquired every 5 min from room temperature to ∼500 K, and every 1 min above ∼500 K. The pressure was monitored and adjusted, in situ, as needed to maintain a constant pressure during the duration of the experiment.

3. RESULTS AND DISCUSSION

3.1. Decomposition of the γ-Phase. To examine the γ-RDX stability, the RDX crystals were compressed to several pressures above 6 GPa and then gradually heated. Raman spectra and optical images were used to monitor changes in the crystals. Typical results from these experiments are shown in Figures 1 and 2. Figure 1, in addition to several Raman spectra

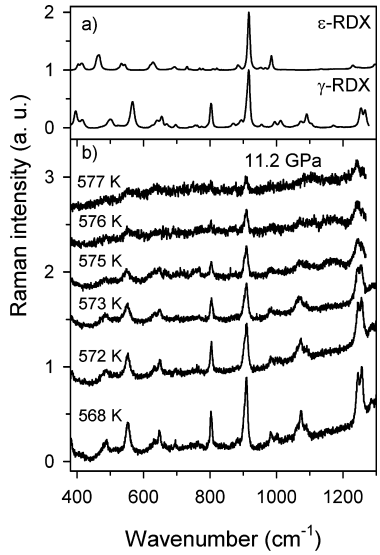

Figure 1. Raman spectra of RDX crystals. (a) γ- and ε-RDX at 11.2 GPa and room temperature. The spectra were acquired over 60 s. (b) γ-RDX at 11.2 GPa and heated at a rate of ∼1 K/min to temperatures indicated. The spectra were acquired over 2 s. All spectra are offset vertically for clarity.

measured at 11.2 GPa and increasing temperatures at a rate of ∼1 K/min, also presents the spectra of γ- and ε-RDX measured at room temperature and 11.2 GPa; the ε-RDX spectrum was obtained on the sample quenched to room temperature.[5] Figure 2 shows crystal images corresponding to the spectra in Figure 1b. Careful examination of changes in Raman peak intensities and sample appearance was used to determine the onset of decomposition. In the presented case, starting at temperatures above ∼570 K a visible decrease in Raman intensity of some peaks and occurrence of marks on the sample surface show clear evidence for the onset of chemical decomposition. Comparisons of the Raman spectra of the decomposing sample with spectra of the γ- and ε-RDX reveal that the decomposition commences and ends in the γ-phase without any involvement of the ε-phase. The same behavior was recorded at other pressures above 6 GPa. Hence, in contrast to previous claims[9] our results demonstrate that the γ-phase of RDX is responsible for its decomposition at HP-HT conditions. The importance of this finding is further investigated and discussed in the next subsections.

3.2. P-T Upper Bound for γ-Phase Decomposition. Experiments were conducted at various pressures to estimate

dx.doi.org/10.1021/jp306589h | J. Phys. Chem. A 2012, 116, 8713−8717

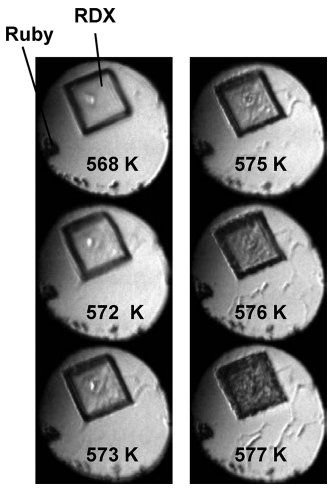

Figure 2. Images of γ-RDX at11.2 GPa and heated at a rate of ~1 K/min to temperatures indicated. Images correspond to the spectra shown in Figure 1. Sample changes indicate the onset of decomposition just below 572 K and completion just above 577 K. The hole diameter in the gasket was ~125 μm.

the upper temperature bound for the γ-RDX decomposition. The results are presented in Figure 3; all of the results were

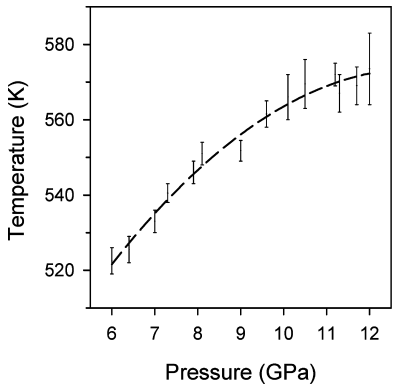

Figure 3. Upper bound of $P-T$ locus for the γ-RDX decomposition. Vertical bars denote the onset and completion of decomposition, as determined from Raman spectra and optical images, during heating at a rate of ~1 K/min. Dashed curve is a least-squares fit to the experimental data.

obtained using a heating rate of ~1 K/min. This rate was selected after examining the effect of heating rates on the decomposition temperature. Tests were performed with higher (3 K/min) and lower (0.1 K/min) rates, which covered the range of rates that fit the thermal response of the high pressure cell. There was almost no difference in the decomposition onset temperature for experiments conducted at 3 and 1 K/min. However, the decomposition onset temperature was more than 10 deg lower for the rate of 0.1 K/min. These results imply that decomposition is kinetically governed, and the data collected at faster heating rates provide the upper bound of the decomposition curve. Because there was no measurable difference in the observed decomposition temperatures for the 1 and 3 K/min rates, we selected the former. This value better matched the thermal response of the cell and was also used in previous studies of RDX.[4]

The results are presented in Figure 3 as the vertical lines, which denote the temperature range over which the decomposition was observed. The beginning and the end of decomposition was estimated from changes in the Raman spectra and sample images, indicated by the decrease of Raman intensity and blackening of the sample. The set of these data approximates the upper bound of temperatures for γ-RDX decomposition. Over the pressure range, 6–12 GPa, examined in this work, the data can be fit to a second order polynomial, $T(P) = 397.85 + 26.7P - 1.01P^2$. The resulting fit is shown in Figure 3 as a dashed curve and can be considered as the demarcation between γ-RDX and its products.

As the γ-RDX approaches, the $P-T$ conditions defined by the curve in Figure 3, it becomes chemically unstable and ultimately decomposes. Therefore, measurements at different $P-T$ can provide insight into the mechanisms governing γ-RDX decomposition. The results of these studies will be presented elsewhere.[15]

3.3. *P–T* Diagram of RDX. In our previous work, we presented the $P-T$ diagram of RDX crystal determined up to ~7 GPa.[4] Here, we extend this diagram by incorporating the results obtained for the γ-RDX at HP-HT. The updated phase diagram is shown in Figure 4. It contains data from ref 4,

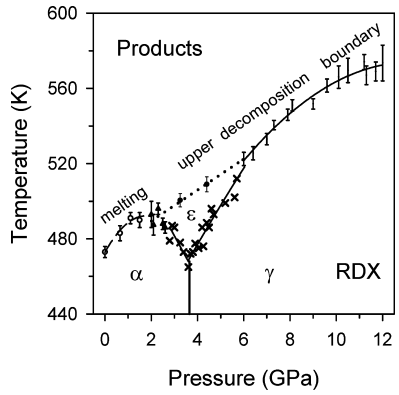

Figure 4. Phase diagram of RDX crystal. Data presented previously in ref 4 and new data for decomposition of ε- and γ-RDX are shown. Symbols and vertical bars of various types denote occurrence/existence of different RDX phases: melting, circles with vertical bars and dashed curve; α-RDX decomposition, solid triangles with vertical bars; $\alpha-\gamma$ phase transition, solid curve; $\alpha-\gamma$ and $\gamma-\varepsilon$ phase transitions, crosses and solid curves; ε-RDX decomposition, solid circles and dotted curve; γ-RDX decomposition, vertical bars and solid curve. All curves represent fits to the experimental data.

current data for γ-phase, and some new data for the ε-phase. Because many aspects of this diagram were discussed in detail before,[4] here we focus primarily on new features. To facilitate the comparison between different phases, only results obtained with the same heating rate of 1 K/min are considered. Because the decomposition was kinetically hindered, this approach was essential for consistent determination of the upper $P-T$ bounds for decomposition.

The experimental data, determining the boundaries between different phases, were fit by a set of curves. It may appear that the upper bound curve for γ-RDX decomposition can be considered as an extension of the decomposition curve for the ε-RDX; however, it has a different slope and the slope decreases with pressure. We also find that the decomposition for both phases is initiated from the solid phase, because there is no evidence for melting before and during decomposition. In contrast, the α-RDX decomposition can apparently originate from either the solid or liquid phase. At the heating rate of 1 K/

dx.doi.org/10.1021/jp306589h | J. Phys. Chem. A 2012, 116, 8713–8717

min, melting of the α-RDX was noticed before the decomposition, dashed curve in Figure 4. However, at a slower heating rate (<1 K/min), α-RDX decomposed from the solid phase before any melting.

The early reports on the formation of ε-RDX indicated that this phase can be produced over a large $P-T$ space.[8,9] In particular, extrapolation of those results to higher pressures suggested that this phase could exist over a broad pressure range and, therefore, dominate the reactive behavior of RDX at HP-HT. In contrast, our recent work[4,5] showed that ε-RDX is formed in a narrow pressure and temperature domain, restricted by the boundaries with the α- and γ-phases, and its own decomposition line.[4,5] However, because all previous studies[4,5,8,9] were performed in a limited $P-T$ range (up to ~7 GPa and 550 K), there was no direct experimental evidence whether the ε-phase can be formed or exist beyond these pressures and temperatures. The current work has addressed this issue, over a larger pressure range (Figure 4) and clearly demonstrated that the ε-phase exists only over a limited $P-T$ region. In other words, updated $P-T$ diagram establishes that the γ-phase, and not the ε-phase, occupies most of the RDX phase diagram. Hence, the γ-phase dominates the behavior of RDX at HP-HT conditions. The consequences of this finding for understanding the changes in shocked RDX crystals are briefly discussed next.

3.4. Relevance of Static Results for Shock Compression. Our previous work on RDX demonstrated that static compression results are useful for elucidating processes under shock compression.[1−3] In particular, changes in the Raman spectra under static compression were used to understand the phase changes in shocked RDX crystals. The $\alpha-\gamma$ phase transition, well established under static compression and recognized by characteristic changes in the Raman spectra at 4 GPa, was shown to occur on nanosecond time scales under shock compression.[1−3]

Here we show that the results obtained from statically compressed γ-RDX can aid in further understanding the processes in shocked RDX. To properly account for shock-induced decomposition of RDX, we need to know the crystal phase at the onset of decomposition. Previous reports speculated that the ε-RDX can be responsible for RDX reactivity under shock conditions.[8,9] We examine this conjecture by comparing the Raman spectra obtained from a shocked, decomposing crystal with the spectra of statically compressed ε- and γ-RDX. The three spectra, measured at comparable pressures, are shown in Figure 5. When comparing these spectra, one should keep in mind that the shocked crystal spectrum was obtained as a time-resolved (approximately nanosecond resolution) spectrum, with a single-pulse laser excitation on a sample undergoing decomposition (details regarding time-resolved measurements under shock compression can be found elsewhere[12]). Thus, this spectrum has a lower signal-to-background ratio than the two other spectra, and the interpretation of the low intensity peaks requires care. Furthermore, peaks in the shocked spectrum are broad due to both thermal broadening and lower spectral resolution of the detection system (in contrast to the resolution of the system used for static measurements). Despite these limitations, it is clear from Figure 5 that the spectrum quality of the shocked crystal is sufficient to make useful comparisons.

Examination of the three spectra reveals several features that can be used to infer similarities between the shocked spectrum and the other two spectra. In the low frequency range, below

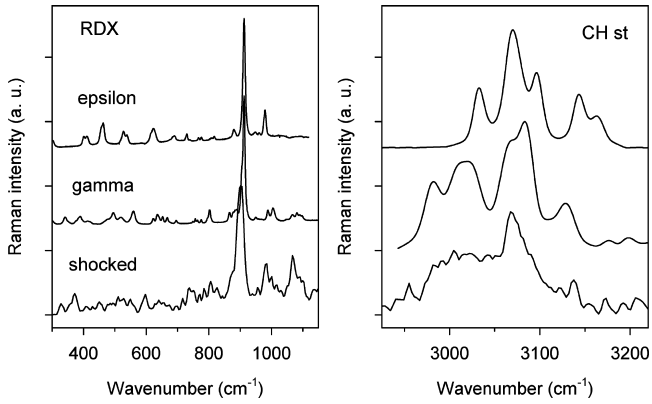

Figure 5. Comparison of Raman spectra of statically compressed γ-RDX and ε-RDX (ref 5) with the spectrum of a shocked RDX crystal (ref 12). The spectra for the ε- and γ-RDX were measured at 9.6 and 9.8 GPa, respectively, and at room temperature. The spectrum of shocked RDX was measured at a peak stress of 10 GPa on a (111) oriented crystal.

1100 cm^{-1}, certain features show strong similarities between the shocked spectra and the γ-phase of statically compressed RDX. Specifically, there are two peaks between 300 and 400 cm^{-1} and peaks around 1080 cm^{-1} that are present in both the shocked crystal and γ-phase spectra, but not in the ε-phase spectrum. Furthermore, the shape of the CH stretching modes, in particular around 3000 cm^{-1}, in the shocked crystal spectrum resembles the γ-phase rather than the ε-phase. Overall, the Raman features provide good evidence that shock-induced decomposition in RDX takes place from the γ-phase but not ε or other phases. This conclusion is consistent with the $P-T$ diagram shown in Figure 4. Because shock induced-decomposition in RDX crystals is observed at stresses above ~5−6 GPa,[12,16] the phase diagram in Figure 4 makes a good case that decomposition starts from the γ-phase. This finding addresses a long lasting question: What is the RDX phase at decomposition? Resolution of this issue is central for modeling the shock-induced decomposition of RDX.

Under shock compression, separating the role of pressure and temperature on decomposition is difficult because the two are coupled. However, the static HP-HT study on γ-phase decomposition has provided important insight into the role of pressure and temperature in the shock-decomposition of RDX. Our previous shock compression studies (reverberation experiments) on RDX showed that the extent of decomposition can be monitored using the light emitted from the decomposing crystal.[12] Subsequently, we found that this light emission increases with the shock stress. Furthermore, the emission rate or the rate of decomposition increases markedly with shock pressure above ~10 GPa, as seen in Figure 6a (adapted from ref 12). Note the spectral resolutions in static and dynamic experiments were 1 and 20 cm^{-1}, respectively. At first glance, this result could suggest that pressure increase is responsible for the observed increase in decomposition rate. However, under shock compression, increase of pressure is also accompanied by an increase of temperature. We have used our HP-HT studies to separate these effects, as discussed below.

The static compression results show that the overall γ-phase decomposition rate decreases with pressure, as shown in Figure 6b. In addition, we have found[15] that the decomposition rates rapidly increase with increasing temperature, at various constant pressures; comprehensive account of γ-phase decom-

dx.doi.org/10.1021/jp306589h | J. Phys. Chem. A 2012, 116, 8713−8717

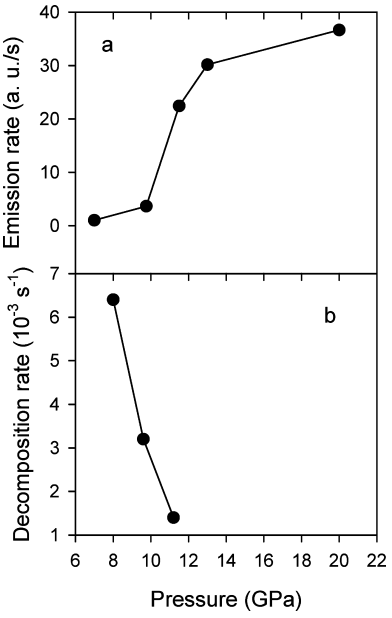

Figure 6. Pressure effects on (a) light emission rate from a shock-compressed decomposing RDX crystal (ref 12) and (b) decomposition rate of statically compressed γ-RDX at 545 K.

position studies will be presented elsewhere.[15] Here, we state that the static compression results reveal that pressure and temperature have opposite effects on the γ-phase decomposition rates: pressure decelerates decomposition whereas temperature accelerates decomposition. This finding has import implication for understanding the observed acceleration of decomposition under shock compression (Figure 6a) and implies that temperature plays the dominant role in this acceleration.

4. SUMMARY AND CONCLUSIONS

Raman spectroscopy and optical imaging in a diamond anvil cell were used to examine the γ-phase of RDX crystals at high pressures and high temperatures to provide new insight into the reactive behavior of RDX at the conditions relevant to shock wave induced decomposition. The Raman and optical imaging results, obtained under static compression from 6 to 12 GPa and temperatures up to 600 K, demonstrate that the γ-RDX, in contrast to previous reports, decomposes at HP-HT conditions without the involvement of other phases. Examination of this phase reactivity provided the $P-T$ upper bound for decomposition and indicated that decomposition decreased with pressure.[15]

Furthermore, we demonstrated that the static compression results obtained for γ-RDX are important for elucidating the decomposition processes under shock compression. By comparing the static results for γ- and ε-phase with the shock compression data,[12] we showed that the shock-induced decomposition of RDX originates from the γ-RDX. Furthermore, the pressure and temperature effects on the decomposition rates of γ-phase under static compression were used to establish that temperature plays the dominant role in the observed acceleration of the RDX decomposition under shock compression.

Finally, this work has extended and complemented our previous studies on polymorphism, stability, phase diagram, and decomposition of RDX under extreme conditions of pressure and temperatures. We have established that among the various RDX phases, the γ-phase plays an important role in the decomposition of RDX under both static and dynamic compression. Therefore, this finding needs to be properly accounted for in RDX reactivity under conditions that are relevant to shock initiation.

AUTHOR INFORMATION

Corresponding Author

*E-mail: dreger@wsu.edu.

Notes

The authors declare no competing financial interest.

ACKNOWLEDGMENTS

Dr. D. E. Hooks from Los Alamos National Laboratory is thanked for providing the RDX crystals. This work was supported by NNSA-DOE Grant DE-NA0000970 and ONR-MURI Grant N00014-06-1-0459.

REFERENCES

(1) Patterson, J. E.; Dreger, Z. A.; Gupta, Y. M. *J. Phys. Chem. B* **2007**, *111*, 10897−10904.
(2) Dreger, Z. A.; Patterson, J. E.; Gupta, Y. M. *J. Phys.: Conf. Ser.* **2008**, *121*, 042012−04015.
(3) Dreger, Z. A.; Gupta, Y. M. *J. Phys. Chem. B* **2007**, *111*, 3893−3903.
(4) Dreger, Z. A.; Gupta, Y. M. *J. Phys. Chem. A* **2010**, *114*, 8099−8105.
(5) Dreger, Z. A.; Gupta, Y. M. *J. Phys. Chem. A* **2010**, *114*, 7038−7047.
(6) Millar, D. I.; Oswald, I. D. H.; Barry, C.; Francis., D. J.; Marshall, W. G.; Pulham, C. R.; Cumming, A. S. *Chem. Commun.* **2010**, *46*, 5662−5664.
(7) Millar, D. I.; Oswald, I. D. H.; Francis, D. J.; Marshall, W. G.; Pulham, C. R.; Warren, J. E.; Cumming, A. S. *Chem. Commun.* **2009**, *5*, 562−564.
(8) Baer, B. J.; Oxley, J.; Nicol, M. *High Pressure Res.* **1990**, *2*, 99−108.
(9) Miller, P. J.; Block, S.; Piermarini, G. J. *Combust. Flame* **1991**, *83*, 174−184.
(10) Karpowicz, R. J.; Sergio, S. T.; Brill, T. B. *Ind. Eng. Chem. Prod. Res. Dev.* **1983**, *22*, 363−365.
(11) Torres, P.; Mercado, L.; Cotte, I.; Hernandez, S. P.; Mina, N.; Santana, A.; Chamberlain, R. T.; Lareau, R.; Castro, M. E. *J. Phys. Chem. B* **2004**, *108*, 8799−8805.
(12) Patterson, J. E.; Dreger, Z. A.; Miao, M. S.; Gupta, Y. M. *J. Phys. Chem. A* **2008**, *112*, 7374−7382.
(13) Miao, M. S.; Dreger, Z. A.; Patterson, J. E.; Gupta, Y. M. *J. Phys. Chem. A* **2008**, *112*, 7383−7390.
(14) Barnett, J. D.; Block, S.; Piermarini, G. J. *Rev. Sci. Instrum.* **1973**, *44*, 1−9.
(15) Dreger, Z. A.; McCluskey, M. D.; Gupta, Y. M. Submitted for publication.
(16) Dang, N. C.; Dreger, Z. A.; Gupta, Y. M.; Hooks, D. E. *J. Phys. Chem. A* **2010**, *114*, 11560−11566.